RSC Advances

ROYAL SOCIETY OF CHEMISTRY

www.rsc.org/advances

Journal Name

ARTICLE

Water-compatible molecularly imprinted polymers prepared using metal-organic gel as porogen

Received 00th January 20xx,
Accepted 00th January 20xx

DOI: 10.1039/x0xx00000x

www.rsc.org/

Li Ma, Lei Tang, Rong-Shan Li, Yan-Ping Huang* and Zhao-Sheng Liu

A novel water-compatible approach suitable for molecular imprinting was described, based on the use of a metal-organic gel (MOG) as porogen. The MOG was synthesised by combining $Fe(NO_3)_3$ and benzene-1,3,5-tricarboxylic acid and used to prepare molecularly imprinted polymer (MIP) containing imprints of levofloxacin with methacrylic acid (MAA) as functional monomer and ethylene glycol dimethacrylate (EDMA) as crosslinkers. Scanning electron microscopy indicated that the MIP and NIP comprised porous microspheres with the sizes from 400 to 800 nm. In contrast, the MIP and non-imprinted polymer (NIP) prepared in the porogen without MOG showed the clusters of polymer rather than beads. In addition, the surface area of the MOG-based MIPs was an order of magnitude larger than that of the MIP without MOG. A detailed study of adsorption experiments confirmed that the MOG-based MIPs showed good recongnition ability in pure water. Polymerization variables, e.g., type of metal ion and coordinating solvents to form MOGs, on the imprinting effect was also investigated. As a conclusion, this approach based on MOG is simple and especially valuable for the domains of the preparation of water-compatible MIPs.

Introduction

Because of their very high selectivity and robustness, molecularly imprinted polymers (MIPs) are being increasingly used as specific recognition materials towards any guest present in any environment.[1] In general, the preparation of MIPs involves the self assembly of functional monomers and target molecules, followed by polymerization in presence of crosslinker to obtain well-defined receptor sites. The polymerization is usually performed in neat organic solvent or solvent mixture to produce macroporoous structure that allows the template access to the imprinted cavities. As a kind of artificial antibodies, MIPs have widely been used for analytical separation,[2] development of assays,[3] construction of chemical sensors,[4] and as enzyme mimics to catalyze chemical reactions.[5]

It is known that the biological receptors have many fascinating characteristics such as outstanding ability of molecular recognition in the aqueous environments. The presently developed MIPs, however, are normally only organic solvent-compatible and mostly fail to show specific binding in the pure aqueous system, which significantly limits their practical applications. This is often due to nonspecific hydrophobically driven binding,[1,4] the extent of which depends on the hydrophobicity of the template and the exposed surface of the material. Recently, some pure water-compatible MIPs have been successfully prepared by adding certain amounts of hydrophilic monomers, e.g., 2-hydroxyethyl methacrylate and acrylamide, in the molecular imprinting processes,[6-8] and their improved surface hydrophilicity proved to be responsible for the water-compatibility. Furthermore, hydrophilic modification on the MIPs surface was another approach to realize the water-compatiblity.[9-11] For example, MIP with hydrophilic polymer brushes can significantly improve their water compatibility by reducing their hydrophobic interactions with template molecules in pure aqueous media.[9]

Although the above methodologies are very simple in principle, the former strategy can only be applied in some special systems; while the latter strategy often involves two-step approach of the surface grafting of hydrophilic polymer layers.[6] Therefore, a facile and general approach is highly desirable for developing water-compatible MIPs.

Metal-organic gels (MOGs), commonly known as coordination polymers, have received considerable research attention from the viewpoint of various practical applications.[12-18] These materials are intrinsically porous in nature and their physicochemical properties can be easily tuned by varying the inorganic and organic counterparts. A typical example in this context is the MOG comprised of Fe ions and terephthalic acid (TPA) or benzene tricarboxylic acid (BTC) ligand. Furthermore, Fe-BTC gel has been successfully utilized to incorporate in situ (without the use of any extraneous oxidant) organic conducting polymers like polypyrrole and polythiophene inside the gel matrix which generated new types of hybrid composite materials. In addition, metal–organic gel has been used as a template for the formation of a macroporous organic polymer.[12-14]

[a] huangyp100@163.com
Tianjin Key Laboratory on Technologies Enabling Development of Clinical Therapeutics and Diagnostics (Theranostics), School of Pharmacy, Tianjin Medical University, Tianjin 300070, China

In this work, we introduce a new approach of molecular imprinting to prepare water-compatible MIPs without need of additional monomers or grafting polymerization. This method is based on the use of MOGs as porogen. The conventional poly(MAA-co-EDMA) system was carried out in the imprinting protocol with water-soluble molecule, levofloxacin (LEFX), as the template. By employing MOGs as porogen, we hereby developed levofloxacin imprinted MIP having (i) the sizes of microspheres from 400 to 800 nm, (ii) the ability of molecular recognition in pure water, and (iii) greater surface that enables the MIPs with higher amount of adsorption. Compared with conventional poly(MAA-co-EDMA) system, the new strategy presented here allows the creation of high-affinity sites in polar mediums since metal ions in MOG may lead to stronger template-monomer interaction by replacing conventional hydrobonding or hydrophobic function with coordination bonding. Polymerization variables, e.g., type of metal ion and coordinating solvents to form MOGs, on the imprinting effect was investigated.

Results and discussion

Preparation of MIP with LEFX imprints in the presence of MOGs

A metal–organic gel with macroscopic structure enables it to be used as a template for the formation of a macroporous organic polymer.[12-14] The gelation of the metal and ligand suggests that there is rapid cross-linking polymerisation between metal ion and H_3BTC, leading to the growth of coordination polymer particles, which themselves subsequently cross-link to leave macroscopic solvent-filled cavities. In this work, H_3BTC was firstly mixed adequately with a certain amount of organic polymer precursor containing methacrylic acid (MAA) and ethylene glycol dimethacrylate (EDMA) in ethanol to make a homogenous solution, which was subsequently mixed with equal volumes of ethanolic solutions containing $Fe(NO_3)_3$ under vigorous stirring. The aerogel displays permanent microporosity with dark orange in colour (Fig. S1). Afterwards, initiating polymerization of the organic monomers was performed to create MOG-based MIP, as shown in Table 1.

To evaluate the selectivity of the resulting MIP based on MOGs, a study screening solvents for rebinding of the template and its analogues was conducted. Binding of LEFX on the MIP (M1) and corresponding NIP in acetonitrile, methanol, ethanol, water and the buffer at different pH of 5.0, 6.8 and 7.4 was investigated. No selectivity was observed in the organic solvents (IF < 1). Interestingly, the MOG-based MIP displayed selectivity in water with an imprinting factor of 1.88.

Table 1 Preparation protocol for levofloxacin-imprinted polymers

Polymer	LEFX (mmol)	MAA (mmol)	EDMA (mmol)	Ethanol (mL)	H_3BTC (mg)	$Fe(NO_3)_3$ (mg)
M1	0.15	1.20	4.80	5.00	100	300
P1	0.15	1.20	4.80	5.00	---	300
P2	0.15	1.20	4.80	5.00	100	---
P3	0.15	1.20	4.80	5.00	---	---
M2	0.15	1.20	4.80	5.00	200	600
M3	0.15	1.20	4.80	5.00	150	450
M4	0.15	1.20	4.80	5.00	50	150
M5	0.15	1.20	4.80	5.00	10	30
P4	0.15	1.20	4.80	5.00	100	190 [a]
P5	0.15	1.20	4.80	5.00	100	173[b]
M6	0.15	1.20	4.80	5.00[c]	100	300
P6	0.15	1.20	4.80	5.00[d]	100	300
P7	0.15	1.20	4.80	5.00[e]	100	300
M7	0.20	1.20	4.80	5.00	100	300
M8	0.12	1.20	4.80	5.00	100	300
M9	0.10	1.20	4.80	5.00	100	300
M10	0.15	1.20	6.00	5.00	100	300
M11	0.15	1.20	8.40	5.00	100	300
M12	0.20	1.60	4.80	5.00	100	300

[a] Cr^{3+}; [b] Cu^{2+}; [c] methanol; [d]: propanol; [e]: dimethyl sulfoxide.

The series of MIPs prepared with MOGs was named with M; the corresponding nonimprinted polymers were named with N. The series of MIPs prepared in absence of MOGs was named with P; the corresponding nonimprinted polymers were named with NP.

As shown in Table S1, the experiment data were fitted with Langmuir mode with correlation coefficients (R^2) of 0.992, indicating that the model fits well in the range of LEFX concentration studied. Scatchard analysis indicated that K_D value of LEFX for high and low selective sites were 0.86 and 2.07 mmol/L, respectively (Fig. S2). The binding capacity of high and low selective sites was 0.34 and 0.44 mmol/g, respectively. In our study, the MOG-based MIP (M1) had a higher heterogeneity index ($1/n$ = 0.43) versus corresponding

NIP (1/*n* = 0.35). However, the LEFX MIP showed little selectivity in the buffer (data not shown) in spite of greater adsorption amount, which suggested the presence of a nonspecific binding between the synthetic receptors and template molecules.[19]

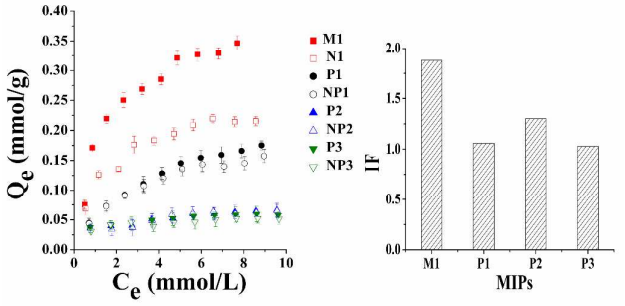

Fig. 1 Imprinting factors and adsorption isotherms of LEFX on the MIPs and NIPs with different of blank controls. *V* = 3.0 mL, C_0 = 0-10 mmol/L, time = 5 h, 20 mg of the polymers. M1: MIP-Fe^{3+}-H_3BTC; N1: NIP-Fe^{3+}-H_3BTC; P1: MIP-Fe^{3+}; NP1: NIP-Fe^{3+}; P2: MIP-H_3BTC; NP2: NIP-H_3BTC. P3: MIP; NP3: NIP.

To probe into the role of MOGs in imprinting, MIP was made in the absence of metal ion. The effect of H_3BTC on imprinting factors was investigated by preparing MIP containing Fe(III) in absence of H_3BTC. The resulting MIP did not show any recognition ability, perhaps due to lower amount of adsorption from smaller specific surface (data not shown) affecting the accessibility of imprinted sites.[21] In addition, MIP made in ethanol in place of MOG as porogen did not show any recognition ability and supported this conclusion. It should be noted that the MOG-based NIP displayed greater adsorption amount than the NIP made with porogen in absence of MOGs (Fig. 1).

To examine weather MOGs participated in the formation of template-functional monomer complex, an NMR study was conducted with a pseudo-pre-polymerization mixture consisting of MOGs composd of Fe(III) and H_3BTC, LEFX, EDMA and MAA. The initiator AIBN was also omitted to avoid the system too complicated to observe complexation between LEFX and MAA. The concentrations of LEFX and MAA were the same as those used in the polymerization of preparing M1. When MAA was added to the solution of LEFX, a peak derived from an amino proton of LEFX exhibited a downfield shift (Fig. S3a), suggesting the formation of hydrogen bonds between LEFX and MAA. Upon the addition of MOGs to the pseudo-pre-polymerization mixture, the carboxyl proton peak of LEFX was observed as a broad peak due to the similar field shift (Fig. S3b). The results strongly suggest that the origin of the imprinting of MOG-based MIP is, at least in part, due to the participatation of MOGs (Fig. S3c and S3d). NMR of pseudo-pre-polymerization mixture including EDMA also approved the obervations above (Fig. S3e and S3f).

Morphologies and characteristics of MOGs-based MIPs

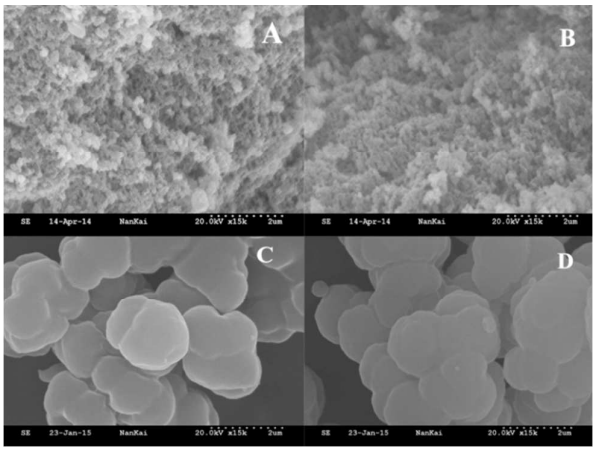

Fig. 2 SEM images of polymers. A: M1, MOG-based MIP; B: N1, MOG-based NIP; C: P3, conventional MIP; D: NP3, conventional NIP.

The scanning electron microscopy (SEM) clearly revealed the different morphologies of the materials. As shown in Fig. 2, MOG-based MIP (M1) and the corresponding control (MOG-based NIP) were found to comprise porous microspheres with the sizes from ca. 400 to 800 nm. In contrast, the MIP and NIP prepared in the porogenic solvent without MOG displayed the clusters of polymer rather beads with 1.6-2 μm. In brief, the use of MOG or not had remarkable influence on the morphology of the resulting polymers. In addition, the SEM of the MOG composed of Fe(III) and H_3BTC in ethanol was conducted, exhibiting a structure of significantly higher density as compared to the MOG-based MIP and NIP (Fig. S4).

Table 2 The surface area, pore volume and pore size of different polymers

Polymers	S_{BET} (m^2g^{-1})	S_t (m^2g^{-1})	V_p ($10^{-3}cm^3g^{-1}$)	D_{mean} (nm)
M1 (Fe^{3+}-H_3BTC)	288.0	227.2	912	13.0
N1 (Fe^{3+}-H_3BTC)	86.9	70.9	294	13.7
P3	2.7	2.7	17.3	22.6
NP3	4.6	4.7	13.6	11.4

MOG-based polymer is expected to have a structure which is a porous "imprint" of the metal–organic gel.[12,13] Multipoint BET measurement was performed to characterize meso-pore of the polymers. As shown in Table 2, all the polymers showed pore diameters almost same size. The BET surface area of MIP-MOG (M1)(288.0 m^2/g) was two orders of magnitude larger than that of the MIP without MOG (P3)(2.7 m^2/g). The exclusion of Fe^{3+}-H_3BTC in the pre-polymerization mixture for MIP P3 and NIP NP3 led to materials with low dry state specific surface areas (P3, 2.7 m^2/g; NP3 4.6 m^2/g), suggesting that the corresponding materials prepared without Fe^{3+}-H_3BTC were essentially nonporous. The BET surface area of NIP-MOG N1(86.9 m^2/g) was also 18 times than that of NIP without MOG (NP3) (4.6 m^2/g). In addition, the MOG-based polymers

displayed "type II" isotherms which are usually related to mesomaterials with pore volume about ten times than that of the the MIP without MOG (Fig. 3). The hysteresis loops resemble H3 types,[20] suggesting that the MIP is porous materials with specific structure of slit-shapes pores. As observed in our previous study, the hysteresis loops were unclosed with a desorption branch that levelled off above the adsorption branch.[21] This effect was previously explained by shrinkage of the polymer when subjected to increasing pressure at the liquid nitrogen temperature.[22]

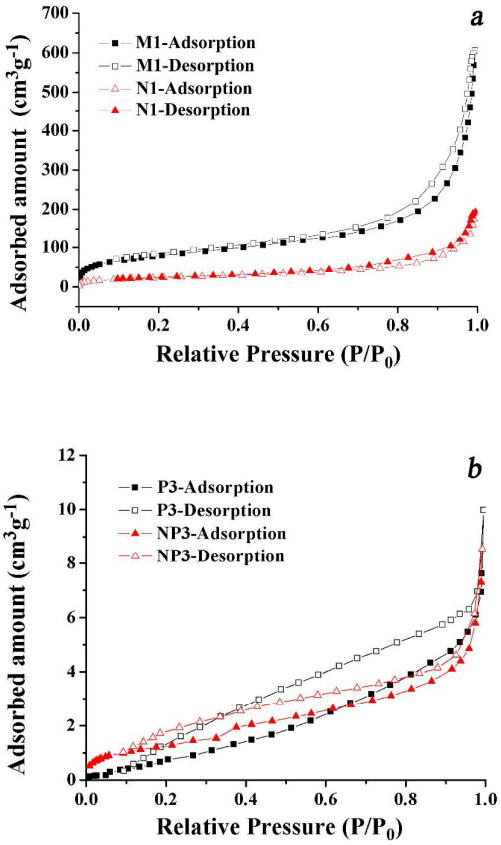

Fig. 3 Nitrogen adsorption-desorption isotherm of MOG-based polymers (M1 and N1) (a) and polymers prepared with MOG-free porogen (P3: MIP; NP3: NIP)(b).

The Fourier-transform infrared (FTIR) spectra of the MIP and NIP are shown in Fig. S5. For both MIP and NIP, characteristic bands are visible at 3452 cm^{-1} (the O–H stretch of the –OH group in MAA), 1729 cm^{-1} (C=O stretch of carboxylic acid in EDMA), and 1673 cm^{-1} (C=O stretch of carboxylic acid in MAA). The peaks at 1264 cm^{-1} and 1144 cm^{-1} were assigned, respectively, to the symmetric and asymmetric ester stretching bands of C–O for EDMA. No characteristic absorption of the template, i.e. the obvious sharp peak at 3476 cm^{-1} (hydroxyl stretch in LEFX), was observed in the spectra of the NIPs, indicating that the template had been successfully removed by the washing process.

Swelling behaviour is known to impact on MIP performance in two ways. Some degree of swelling facilitates template access to the specific binding cavity within the MIP. However, high levels of swelling can lead to cavity deformation reducing the matching degree of the template and cavity.[23] Typically polymers prepared in solvating porogens will experience a greater dynamic swelling range due to a decreased crosslinking network.[19] This results from later phase separation of the growing polymer chains, resulting in a lower degree of aggregation of the polymer particles. Therefore, the differences in swelling is related to the heterogeneity of the cross-link density, which in turn will affect the rigidity of the chains linking the agglomerates or microspheres together during phase separation.

The degree of MIP swelling was determined in ethanol, the co-solvent to form MOG. The MOG-based MIP (M1) showed approximately 11.93 % swelling, lower than the MOG-based NIP (N1) (14.60 %) (Table S2). It should be noted that the MOG-based MIP and NIP showed a similar pattern of swelling behaviour in water or PBS buffer (pH 7.40). The order of swelling behavior was opposite to that of pore volume of polymer, which was in agreement with the work of Sellergren and Shea.[22] In contrast, the MOG-free MIP (P3) showed higher swelling than the MOG-free NIP (NP3). This is most likely attributed to the shift of polymerization rate in MOG or non-MOG solvent which may naturally affect the buildup of the pore structure. Secondly, the increase in solvent viscosity with MOG as porogenic solvent is also likely to influence the gelation process prior to phase separation. In addition, minimal differences were noted between the MIPs and NIPs made in absence of MOG. In view of the higher swelling of the MOG-based polymers compared to the MOG-free polymers, it appears that MOG is good solvent for MAA-EDMA polymer which more efficiently solvates the growing polymer chains.

Adsorptive characteristics of MOGs-based MIPs

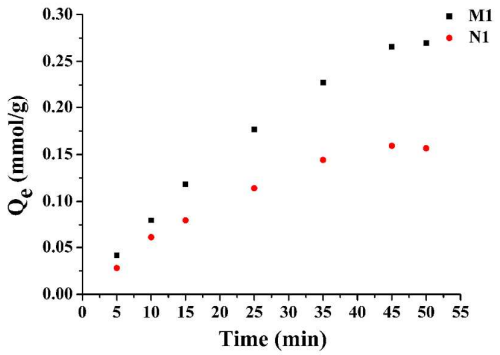

Fig. 4 Kinetic binding of LEFX on the M1 (MOG-based MIP) and N1 (MOG-based NIP). The dried polymer particles of 20 mg were placed in a 5-mL centrifugal tube and mixed with 3.0 mL of LEFX solution with concentration of 7.0 mmol/L.

Adsorption kinetics of materials is indicator of adsorption efficiency (Fig. 4). As illustrated in Table S3, the pseudo

second-order model was more suitable to describe the adsorption kinetic data for LEFX bound onto the MIP-MOG and NIP1-MOG. For the MIP1-MOG, Q_e and k_2 were calculated to be 0.53 mmol g^{-1} and 3.63×10^{-2} g $mmol^{-1}min^{-1}$, respectively. For the NIP1-MOG, Q_e and k_2 were calculated to be 0.25 mmol g^{-1} and 1.27×10^{-1} g $mmol^{-1}min^{-1}$, respectively. k_2 of the MIP-MOG was higher than that of the NIP-MOG, indicating that the chemisorption might not be the rate-limiting step controlling binding process of LEFX.[24]

To demonstrate the role of metal ion in imprinting of MOG-based MIP, adsorption experiment was also performed in a water solution of $Fe(NO_3)_3$ with identical concentration to that in polymerization recipe. The result showed that the adsorption amount of the MIP and NIP were all decreased (Fig. S6). However, imprinting factor increased (IF = 3.2) due to the suppressing of non-selective sites of the NIP in the solution of $Fe(NO_3)_3$. Obviously, the metal ion to form MOG participated in the molecular recognition in the MOG-based MIP. This situation is similar to previously reported work based to metal ion as pivot in imprinting.[25] In addition, the heterogeneity index ($1/n$ = 0.58) of the MOG-based MIP (M1) increased while the heterogeneity index of the MOG-based NIP remained unchanged in $Fe(NO_3)_3$ solution.

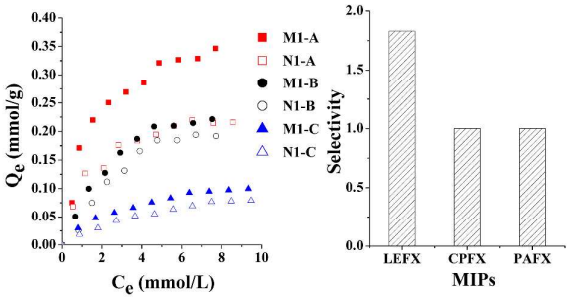

Fig. 5 Imprinting factors and adsorption isotherms of LEFX and analogues on the MIPs and NIPs. V = 3.0 mL, C_0 = 0-10 mmol/L, time = 5 h, 20 mg of the polymers. A: LEFX is the template; B: CPFX; C: PZFX. CPFX and PZFX are analogues.

Fig. 5 indicates the cross-reactivity, i.e., the ability of recognizing not only the template in the rebinding step but also structurally related analytes,[26] of polymers imprinted by LEFX by investigating rebinding of the template and its analogues in methanol. MOG-based MIP particles (M1) were 1.80, and 1.09 times more selective than the corresponding NIP particles for ciprofloxacin, and pazufloxacin, respectively. This observation suggested that the analogues cannot bind as strongly as LEFX. It seemed that the quinolones-like unit of these molecules are hardly trapped in LEFX cavities in the MOG-based MIP, probably due to mismatching between the analogues size and the size of the cavities or the position of their functional groups and the position of the functional groups in cavities.

The binding affinities of the MOG-based MIP (M1) were further examined for a series of water soluble compounds (Fig. S7). These compounds differed in shape, distribution of functionality and number of binding points. For CAP and CTRZ, little affinity of the MOG-based MIP to the two molecule was observed. For 5-FU, some affinities can be achieved due to nonspecific H-bandings between 5-FU and randomly incorporated functional groups.

Effect of polymerization variables on affinity of MOGs-based MIP

Ratio of template to functional monomer

The influence of template-monomer (T/M) molar ratio on the imprinting factor of the resultant MIP (M7-M9) was studied because the molar relationship between the monomer and template has been found to be important with respect to the number and quality of recognition sites in MIPs.[27,28] On the one hand, more imprinting sites can be obtained as the increase in the amount of the template. On the other hand, the excess of monomer would yield high numbers of non-complexed, randomly distributed monomer and more non-specific binding sites, which contribute to decreasing imprinting factor. The greatest imprinting factor was obtained on M1, which was prepared with a T/M ratio of 1:8 (Fig. S8). A possible explanation for this was that a balance of two effect was achieved. Further increase in T/M ratio (1/12) led a decrease in imprinting effect (IF < 1), which may be fewer imprinted sites on the MIP.

Type of metal ion

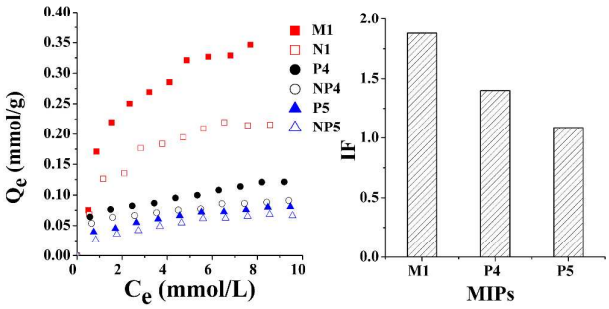

Fig. 6 Imprinting factors and adsorption isotherms of LEFX on the MIPs and NIPs with different kinds of ions. V = 3.0 mL, C_0 = 0-10 mmol/L, time = 5 h, 20 mg of the polymers. M1: MIP-Fe^{3+}; N1: NIP-Fe^{3+}; P4: MIP-Cr^{3+}; NP4: NIP-Cr^{3+}; P5: MIP-Cu^{2+}; NP5: NIP-Cu^{2+}.

To understand the effect of reaction conditions on the imprinting of MOGs-based MIP, other metal precursor salts containing Cu(II), Cr(III), Zn (II) and Ni (II) were examined to prepare MOGs. Unlike $Fe(NO_3)_3{\cdot}9H_2O$, the reaction between $Zn(NO_3)_2{\cdot}6H_2O$ and $Ni(NO_3)_2{\cdot}6H_2O$ did not result in the formation of gel material. The rebinding data highlighted the effects of metal ion on the MOG MIP systems. The highest imprinting factor was achieved in Fe(III)-based MOG (IF = 1.88) (Fig. 6). In contrast, Cr(III) and Cu(II)-based MOG showed imprinting factor of 1.27 and 1.11, respectively.

Previous studies have shown that introduce of metal ion in the pre-polymerization systems yielded MIPs with enhanced affinity.[29-32] For example, Zhao et al found the retention factor of template in metal ion-based MIP to be five fold than metal ion-free MIP.[29] The Liu's group synthesized mandelic acid-imprinted polymers with Co(II) to achieve the chiral separations.[30] Finally, Li et al showed that metal ion as pivot results in a higher capacity factor for MIP prepared with macromonomers.[31] Presumably, metal ions in MOG are ultimately responsible for the creation of high-affinity sites.[32] This can be demonstrated by the lost of imprinting effect of the resulting MIP eluting with ionic complexing agent, ethylene diamine tetraacetic acid (EDTA) to remove the metal ion thoroughly.

Coordinating solvent

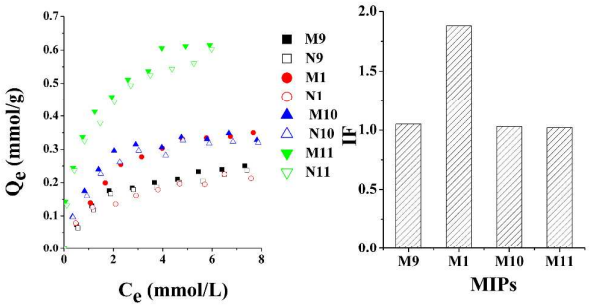

Fig. 7 Imprinting factors and adsorption isotherms of LEFX on the MIPs and NIPs with different kinds of solvent. V = 3.0 mL, C_0 = 0-10 mmol/L, time = 5 h, 20 mg of the polymers. M6: MIP-methanol; N6: NIP-methanol; M1: MIP-ethanol; N1: NIP-ethanol; P6: MIP-propanol; NP6: NIP- propanol; P7: MIP-DMSO; NP7: NIP-DMSO.

The various organic solvents such as ethanol, DMSO, propanol and acetone were also chosen as the coordinating solvents to prepare MOGs. In the case of Fe^{3+}, methanol, ethanol, propanol and DMSO could rapidly give coordination gels at ambient temperature, whereas acetone and acetonitrile led to the precipitates. The effect of MOGs formed with different solvent on the affinity and recognition ability of the MIP as further studied (Fig. 7). When the coordinating solvent was DMSO, the greatest adsorption to the template was found on MIP P7. However, the corresponding NIP (NP7) also indicated high adsorption amount for the template. As a result, negligible imprinting effect was observed for MIP made with DMSO as the coordinating solvent. Similar amount of adsorption to the template on the MIP and NIP prepared with methanol or propanol as the coordinating solvent was also found. In contrast, obvious difference in adsorption amount for the template on the MIP and NIP prepared with ethanol was observed with imprinting factor of 1.88.

The impact of changing the total monomers to porogenic solvent ratio on the imprinting effect of the resulting MIPs was studied, whereas the porogenic solvent was increased from 79.3% to 81.9% (w%)(Fig. 8). It was found that the ratio of 80.6% MOG in pre-polymerization led to the MIP with the greatest imprinting effect in terms of imprinting factor. Contrary to the polymers prepared in conventional porogen, the MIPs prepared using MOG as porogen showed selectivity dependence on the MOG composition and the synthesis conditions. Various factors related to the physical characteristics of the polymers, such as swelling and surface charge, should be contributing factors driving this selectivity.[28]

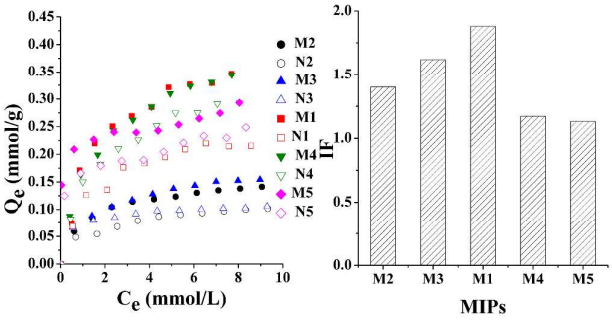

Fig. 8 Imprinting factors and adsorption isotherms of LEFX on the MIPs and NIPs with different amount of ratio of MOGs to monomers. V = 3.0 mL, C_0 = 0-10 mmol/L, time = 5 h, 20 mg of the polymers. M2, N2: W_{MOGs} = 81.9%; M3, N3: W_{MOGs} = 81.2%; M1, N1: W_{MOGs} = 80.6%; M4, N4: W_{MOGs} = 79.9%; M5, N5: W_{MOGs} = 79.3%.

The impact of changing the total monomers to porogenic solvent ratio on the imprinting effect of the resulting MIPs was studied, whereas the porogenic solvent was increased from 79.3% to 81.9% (w%)(Fig. 8). It was found that the ratio of 80.6% MOG in pre-polymerization led to the MIP with the greatest imprinting effect in terms of imprinting factor. Contrary to the polymers prepared in conventional progen, the MIPs prepared using MOG as porogen showed selectivity dependence on the MOG composition and the synthesis conditions. Various factors related to the physical characteristics of the polymers, such as swelling and surface charge, should be contributing factors driving this selectivity.[28]

Ratio of functional monomer to cross-linking monomer

It is well known that the decisive factor for high selectivity is the quantity of cross-linking monomer used in the production of MIPs.[1,19] For the non-covalent approach, the relationship between the cross-linking (CL) degree of the polymers and its recognition property is rather complicated. In a few cases, selectivity of the resulting MIPs increases as the increase in levels of crosslinker.[33] In another case, the selectivity reached to a maximum at one lower degree of cross-linking.[34] In present study, it was found that the cavities in lesser cross-linked matrixes (CL percentage of 75%) have lower imprinting factor due to the greater flexibility of the matrix (Fig. S9). Changing the apparent CL percentage from 80% to 83% resulted in the most noticeable shift in the adsorption amount of the template for the both the MIPs (M10-M12) and NIPs. It was found that the best apparent CL percentage was 80% in

terms of imprinting factor. Further increase in levels of crosslinker (85%) led a rapid decrease in imprinting effect (IF < 1), with greater adsorption amount of the template for the NIP than the MIP. The result suggested that high levels of crosslinker might lead to the stiffness of the polymer network increased severely in consideration of almost constant adsorption capacity to the MIP with CL percentage of 80%, thus decrease the accessibility of the cavities significantly.

Application of MOG-based MIPs: Drug release

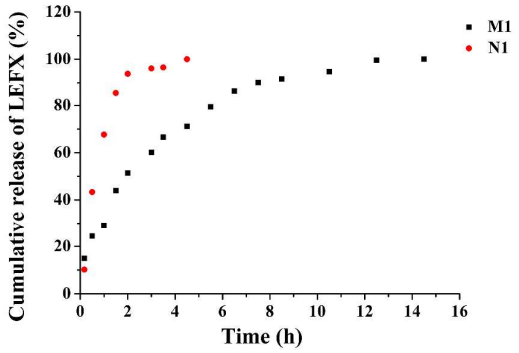

Fig. 9 Release profile of LEFX from M1 and N1 in PBS (pH 6.80)

The release profiles of LEFX from the MOG-based MIP and NIP are depicted in Fig. 9. The release of LEFX in pH 6.8 (simulated intestinal fluid) at room temperature from control polymers was very rapid, about 85% occurring in the first hour. In the case of the MIP, sustained release effect was observed and the release of LEFX was prolonged over a period of 12 h. This observation can be attributed to the hypothesis that the presence of specific binding sites in the polymer matrix provides superior controlled release characteristics.

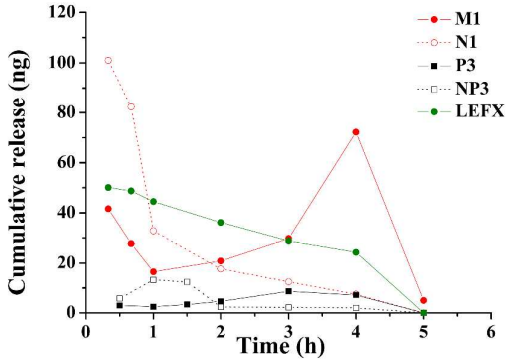

Fig. 10 Pharmacokinetic profiles of LEFX in rats receiving an oral dosing of 250 μg LEFX drug-loaded M1 and N1, the blank control P3 and NP3. M1, MOG-based MIP; N1, MOG-based NIP; P3, conventional MIP; NP3, conventional NIP.

Fig. 10 shows the plasma concentration versus time following application of the MOG-based polymers containing LEFX and direct application of the conventional polymers containing LEFX or the pure LEFX alone (the controls). The plasma concentration levels of LEFX increased markedly and reached the maximum concentration within 4 h after applying the MOG-based MIP (Fig. 10). The release rate of LEFX of the MOG-based MIP was lower for both conventional MIP and conventional NIP, which was reflected by the longer time to maximum plasma concentration (T_{max}). The maximum plasma concentration (C_{max}), which is relative to drug action and usually used to assess the bioequivalence, of the MOG-based MIP was about 7 times higher than that of the conventional MIP, and was about 5 times higher than that of the conventional NIP (Fig. 10). In contrast, the MOG-based NIP containing LEFX and pure LEFX did not show the maximum plasma concentration of LEFX. The results indicated that the degree of drug release in vivo achieved using the MOG-based NIP containing LEFX could result in considerably higher therapeutic advantage.

Experimental

Materials and instruments

Levofloxacin (LEFX) was from Hubei Hengshuo Pharmaceutical Co., Ltd. (98.0%, Hubei, China). Methacrylic acid (MAA) was purchased from Kermel Chemical Reagent (99.0%, Tianjing, China). Ethylene glycol dimethacrylate (EDMA) was from Sigma (98.0%, USA). 2,2-Azobis (butyronitrile) (AIBN) were supplied by Kermel Chemical Reagent (98.0%, Tianjin, China). 1,3,5-Benzenetricarboxylic acid (H_3BTC) were from J&K (99.0%, Beijing, China). $Fe(NO_3)_3{\cdot}9H_2O$ were obtained from Kermel Chemical Reagent (98.5%, Tianjing, China). Capecitabine (CAP, 99.5 %), ciprofloxacin (CPFX, 99.5 %) and pazufloxacin (PZFX, 99.5 %) were supplied by Dalian Meilun Biological technology Co., Ltd. (Dalian, China). Cetirizine (CTRZ) was from Hubei Hengshuo Pharmaceutical Co., Ltd. (98.0%, Hubei, China). 5-Fluorouracil (5-FU) was purchased from J&K (99.0%, Beijing, China). Citric acid (HPLC grade) was supplied by Kermel Chemical Reagent (99.8%, Tianjin, China). Acetonitrile (HPLC grade) was purchased from Biaoshiqi Science & Technology Development Co., Ltd. (99.9%, Tianjing, China). Other analytical reagents were from Jiangtian Chemical Reagent Co. Ltd. (Tianjin, China).

Preparation of MOG-based molecularly imprinted polymers

MOG-based MIPs were prepared by situ preparation using the Fe^{3+}–H_3BTC metal–organic hybrid gel as coordination porogen. LEFX and H_3BTC were firstly mixed with MAA and EDMA in ethanol to make a homogenous solution, which was subsequently mixed with equal volumes of $Fe(NO_3)_3$ dissolved in ethanol, in a 10 mL glass ampoule. After ultrasonic sound of 10 min, the ampoule was sealed and the mixture was kept at 65 °C for 24 h. The obtained polymers were ground into fine powder, and washed by Sechelt extractor using methanol-acetic acid mixture (90:10, v:v) for three days, followed by methanol for another one day, until the template, unreacted monomers could no longer be detected by UV

spectrophotometer. Then the polymers were vacuum dried. NIPs were made in the same manner except LEFX was not included in the formulation.

Adsorption experiments

The binding capacity of MIPs and NIPs for LEFX were analyses as follows. Typically, LEFX dissolved in water of 10 mmol/L was first prepared. Then the solution was diluted to different concentrations (1-10 mmol/L) with water for detection. 20 mg of MIPs and NIPs were immersed in 3.00 mL of water with a known concentration of LEFX (1-10 mmol/L). After shaking five hours at room temperature, samples were centrifuged for 5 min (8,000 rpm) and the LEFX concentration in the supernatant was measured using UV-visible spectrophotometer at 294 nm. The loading capacity of polymers was calculated by subtracting the amounts of free drug from its initial value according to the following equation:[20]

$$Q_e = \frac{(C_0 - C_e) \times V}{M} \quad (1)$$

where Q_e (mmol/g) is the binding capacity of polymers; C_0 and C_e (mmol/L) are the initial and equilibrium concentration, respectively; V (mL) is the volume of solutions; and M (mg) is the mass of the polymers added to the solutions.

Langmuir model is used to characterize the MIPs as follows:[28]

$$Q_e = \frac{Q_{max} K C_e}{1 + K C_e} \quad (2)$$

where Q_e is the amount of LEFX adsorbed at equilibrium (mmol/g), Q_{max} is the amount of LEFX adsorbed for a complete monolayer (mmol/g), C_e is the equilibrium concentration (mmol/L), and K is a Langmuir constant related to the energy or net enthalpy of sorption (L/mmol).

The Freundlich isotherm is used to describe the surface heterogeneity of MIPs:[28]

$$Q_e = k_F C_e^{1/n} \quad (3)$$

k_F {(mg/g)(mg/L)-1/n} is a Freundlich constant related to the adsorption capacity; 1/n is a heterogeneity index depicting the surface heterogeneity of sites, ranging from 0 to 1.

Scatchard model is often used to characterize the binding parameters of high affinity and low affinity binding sites in MIPs due to curved Scatchard plots:[30]

$$\frac{Q_e}{C_e} = \frac{Q_{max} - Q_e}{K_d} \quad (4)$$

where K_d (mmol/L) is the equilibrium dissociation constant.

Imprinting effect of the MIPs is assessed with imprinting factor (IF), which was defined as:[35]

$$IF = Q_{MIP} / Q_{NIP} \quad (5)$$

where Q_{MIP} and Q_{NIP} is the amounts of bound template on the MIP and the non-imprinted polymer (NIP), respectively.

Kinetic adsorption experiments

The adsorption kinetics was studied by monitoring the amounts of LEFX in the solutions at different incubation times (5-120 min). The dried polymer particles (20 mg) were placed in a 5-mL centrifugal tube and mixed with 3.0 mL of LEFX solution with concentration of 7.0 mmol/L. The mixtures were shaken at room temperature for different time, and then centrifuged at 8,000 rpm for 3 min.

The pseudo-second-order model was used to characterize the MIPs/NIPs assuming adsorption as the rate-controlling step:[20]

$$Q_t = \frac{t k_2 Q_e^2}{1 + t k_2 Q_e} \quad (6)$$

where t is the adsorption time (s), Q_t is the amounts of template adsorbed at time t (mmol/g), and k_2 is the adsorption rate constant of pseudo-second-order model [(mmol/g)s^{-1}].

Drug release experiments *in vitro*

The imprinted or corresponding non-imprinted materials of 80 mg were immersed in 8 mL of definite LEFX concentrations solution for 3 days to get loaded MIPs and NIPs. Before use, the solution containing polymers and LEFX were centrifuged, washed with ethanol for three times and dried at room temperature.

In order to investigate the drug release behaviour in vitro, PBS solutions of specific pH values were used as the release medium. 70 mg of the loaded MIP and NIP materials were suspended in 200 mL of the buffer solution, and the stirring rate was maintained at 50 rpm/min. Samples from the solution medium were withdrawn periodically and analyzed using HPLC-UV. Fresh PBS aqueous solution with the same volumes were added into the release medium to maintain a constant volume of the solution.

Drug release experiments *in vivo*

The controlled-released effects of the MOGs-based MIPs and NIPs were also demonstrated by in vivo drug-release assay in Wistar rats. In each individual test, four male, 2-months-old NMRI mice (with a weight of approx. 200 g) were intragastric administration MIPs (100 mg) uploaded with 200 μg of LEFX which were suspended in 1.50 mL normal saline. Other polymers with the same quality were given to the rats as well. Due to the high content of LEFX, the commercial medicine was reduced to 0.8 mg for comparison. Blood samples (100 μL) were withdrawn at different time intervals from the femoral vein of Wistar rats. Samples were centrifuged (13,000 rpm, 5 min) to get plasma samples, and then stored in tube at -20°C if not used immediately.

LEFX contained in rat plasma from oral suspension and in tablet dosage form was measured by HPLC. The plasma samples (50 μL) were added with 150 μL acetonitrile to precipitate protein, followed by centrifuged to produce the analytes containing LEFX. The solution was dried by nitrogen at room temperature. Residues were reconstituted by 50 μL mobile phase, and then subjected to HPLC. Analysis was

performed by an Agilent 1100 system, which consisted of a G1311A pump, a G1322A degasser, a G131513 DAD detector, a Rheodyne 7225 injector with a 20 μL loop, and a Vertex VT4820 temperature controller. Data processing was carried out with a HPCORE workstation. The detection was set at 294 nm and the column temperature was kept at 25°C. Chromatographic column was 100-5C18 (4.6 × 250 mm, Kromasil, Sweden). Mobile phase was 50 mM citric acid (pH 4.0): acetonitrile (85:15, v/v) with flow-rate of 1.0 mL/min. The detection limit was 10.0 ng/μL for LEFX.

Conclusions

In this work, we have successfully prepared MIPs with MOG as porogenic solvent. Two of polymerization variables are key factor in affecting imprinting effect, i.e., type of metal ion and coordinating solvents. It was found that metal ions contribute to enhanced imprinting for the imprinted polymer based on MOG. Compared to the imprinted polymers prepared with other traditional porogens, the MIP reported here indicated greater specific surface areas. The good water compatibility of the MOG-based MIP was demonstrated by investigating the molecular recognition ability of the MIP in water. In summary, using MOGs as porogenic solvent may be a promising approach for the MIPs of water compatibility without need of additional monomers or grafting polymerization.

Acknowledgements

This work was supported by the National Natural Science Foundation of China (Grant No. 21375096).

Notes and references

1 B. Tóth, and G. Horvai, *Top Curr. Chem.*, 2012, **325**, 267.
2 C. Zheng, Y. P. Huang, and Z. S. Liu, *Anal. Bioanal. Chem.*, 2013, **405**, 2147.
3 R. Schirhagl, *Anal. Chem.*, 2014, **86**, 250.
4 T. P. Huynh, and W. Kutner, *Biosens. Bioelectron.*, 2015, **74,** 856.
5 G. Wulff, and J. Liu, *Acc. Chem. Res.*, 2012, **45**, 239.
6 B. Dirion, Z. Cobb, E. Schillinger, L. I. Andersson, and B. Sellergren, *J. Am. Chem. Soc.*, 2003, **125**, 15101.
7 Z. Cobb, B. Sellergren, and L. I. Andersson, *Analyst,* 2007, **132**, 1262.
8 E. Benito-Pena, J. L. Urraca, B. Sellergren, and M. C. Moreno-Bondia, *J. Chromatogr. A*, 2008, **1208**, 62.
9 G. Pan, Y. Zhang, Y. Ma, C. Li, and H. Zhang, *Angew. Chem. Int. Ed.*, 2011, **50,** 11731.
10 S. Xu, H. Lu, and L. Chen, *J. Chromatogr. A*, 2014, **1350**, 23.
11 Y. Ma, G. Pan, Y. Zhang, X. Guo, and H. Zhang, *Angew. Chem. Int. Ed.*, 2013, **52**, 1511.
12 Q. Wei and S. L. James, *Chem. Commun.*, 2005, 1555.
13 J. Yin, G. Yang, H. Wang and Y. Chen, *Chem. Commun.*, 2007, 4614.
14 F. Yang, Z. Lin, X. He, L. Chen, Y. Zhang, *J. Chromatogr. A*, 2011, **1218**, 9194.
15 W. L. Leong, A. Y. Y. Tam, S. K. Batabyal, L. W. Koh, S. Kasapis, V. W. W. Yam and J. J. Vittal, *Chem. Commun.*, 2008, 3628.
16 S. Xiang, L. Li, J. Zhang, X. Tan, H. Cui, J. Shi, Y. Hu, L. Chen, C.-Y. Su and S. L. James, *J. Mater. Chem.*, 2012, **22**, 1862.
17 S. Barman, J. A. Garg, O. Blacque, K. Venkatesan and H. Berke, *Chem. Commun.*, 2012, **48**, 11127.
18 M. R. Lohe, M. Rose and S. Kaskel, *Chem. Commun.*, 2009, 6056.
19 B. Sellergren, *J. Chromatogr. A*, 2001, **906**, 227.
20 K. S. W. Sing, *Pure Appl. Chem.*, 1982, **54**, 2201.
21 X.-Y. Li, X.-X. Chen, D.-D. Zhong, Y.-P. Huang and Z.-S. Liu, *RSC Adv.*, 2014, **4**, 50662.
22 B. Sellergren and K. J. Shea, *J. Chromatogr. A,* 1993, **635**, 31.
23 D. Spivak, *Adv. Drug Deliv. Rev.*, 2005, **57**, 1779.
24 Y. Ren, W. Ma, J. Ma, Q. Wen, J. Wang, and F. Zhao, *J. Colloid Interface Sci.*, 2012, **367**, 355.
25 S. J Li, C. Liao, W. Li, Y. Chen, and X. Hao, *Macromol. Biosci.*, 2007, **7,** 1112.
26 C. J, Allender, K. R. Brain, and C. M. Heard, *Chirality,* 1997, **9**, 233.
27 H. S. Andersson, J. G. Karlsson, S. A. Piletsky, A.-C. Koch-Schmidt, K. Mosbach, and I.A. Nicholls, *J. Chromatogr. A*, 1999, **848**, 39.
28 A. M. Rampey, R. J. Umpleby II, G. T. Rushton, J. C. Iseman, R. N. Shah, and K. D. Shimizu, *Anal. Chem.,* 2004, **76**, 1123.
29 L. Zhao, L. Ban, Q.W. Zhang, Y. P. Huang, and Z. S. Liu, *J. Chromatogr. A*, 2011, **1218**, 9071.
30 X.-Y. Li, L. Ma, Y.-P. Huang, Z.-S. Liu and H. A. Aisa, *RSC Adv.*, 2015, **5**, 36753.
31 L.-H. Bai, X.-X. Chen, Y.-P. Huang, Q.-W. Zhang and Z.-S. Liu, *Anal. Bioanal. Chem.*, 2013, **405,** 8935.
32 D.-D. Zhong, Y.-P. Huang, X.-L. Xin, Z.-S. Liu, and H. A. Aisa, *J. Chromatogr. B*, 2013, **934**, 109.
33 C. Yu, and K. Mosbach, *J. Chromatogr. A*, 2000, **888**, 63.
34 A.G. Mayes, and K. Mosbach, *Anal. Chem.*, 1996, **68,** 3769.
35 C. I. Lin, A. K. Joseph, C. K. Chang, Y. C. Wang, and Y. D. Lee, *Anal. Chim. Acta*, 2003, **481,** 175.